

An ionogram plot showing two distinct traces of ionospheric data against a dark blue background with a grid of lighter blue lines. The traces are yellow and green, curving upwards from left to right.

# RAPPORTI TECNICI INGV

IonoNet: the INGV ionosonde network  
for oblique soundings



ISTITUTO NAZIONALE DI GEOFISICA E VULCANOLOGIA

491

**Direttore Responsabile**

Daniela VERSACE

**Editor in Chief**

Milena MORETTI (editorinchief.collane-editoriali@ingv.it)

**Editorial Board**

Laura ALFONSI (laura.alfonsi@ingv.it)  
Christian BIGNAMI (christian.bignami@ingv.it)  
Simona CARANNANTE (simona.carannante@ingv.it)  
Viviana CASTELLI (viviana.castelli@ingv.it)  
Luca COCCHI (luca.cocchi@ingv.it)  
Luigi CUCCI (luigi.cucci@ingv.it)  
Lorenzo CUGLIARI (lorenzo.cugliari@ingv.it)  
Alessia DI CAPRIO (alessia.dicaprio@ingv.it)  
Roberto DI MARTINO (roberto.dimartino@ingv.it)  
Domenico DI MAURO (domenico.dimauro@ingv.it)  
Domenico DORONZO (domenico.doronzio@ingv.it)  
Filippo GRECO (filippo.greco@ingv.it)  
Alessandro IAROCCI (alessandro.iarocci@ingv.it)  
Mario MATTIA (mario.mattia@ingv.it)  
Daniele MELINI (daniele.melini@ingv.it)  
Anna NARDI (anna.nardi@ingv.it)  
Lucia NARDONE (lucia.nardone@ingv.it)  
Marco OLIVIERI (marco.olivieri@ingv.it)  
Pierangelo ROMANO (pierangelo.romano@ingv.it)  
Maurizio SOLDANI (maurizio.soldani@ingv.it)  
Sara STOPPONI (sara.stopponi@ingv.it)  
Umberto TAMMARO (umberto.tammaro@ingv.it)  
Andrea TERTULLIANI (andrea.tertulliani@ingv.it)  
Stefano URBINI (stefano.urbini@ingv.it)

**Ufficio Editoriale**

Francesca DI STEFANO - Coordinatore - Segreteria di Redazione

**Produzione e grafica-redazionale**

Barbara ANGIONI  
Massimiliano CASCONI  
Francesca DI STEFANO  
Patrizia PANTANI

**REGISTRAZIONE AL TRIBUNALE DI ROMA N.174 | 2014, 23 LUGLIO**

© 2014 INGV Istituto Nazionale di Geofisica e Vulcanologia | Rappresentante legale: Carlo DOGLIONI

Sede: Via di Vigna Murata, 605 | Roma



ISTITUTO NAZIONALE DI GEOFISICA E VULCANOLOGIA

# RAPPORTI TECNICI INGV

## IonoNet: the INGV ionosonde network for oblique soundings

Achille Zirizzotti<sup>1</sup>, Umberto Sciacca<sup>\*1</sup>, Enrico Zuccheretti<sup>1</sup>, James Arokiasamy Baskaradas<sup>2</sup>,  
Giuseppe Tutone<sup>1</sup>, Giovanni Benedetti<sup>1</sup>

<sup>1</sup>INGV | Istituto Nazionale di Geofisica e Vulcanologia, Sezione Roma 2

<sup>2</sup>School of EEE, SASTRA Deemed to be University, Tamil Nadu, India, Associato di ricerca INGV

*\*Corresponding author*

Accepted 19 December 2024 | Accettato 19 dicembre 2024

How to cite | Come citare Zirizzotti A., Sciacca U., Zuccheretti E., Arokiasamy B.J., Tutone G., Benedetti G., (2025). IonoNet: the INGV ionosonde network for oblique soundings. Rapp. Tec. INGV, 491: 1-28, <https://doi.org/10.13127/rpt/491>

Cover Ionogram, detail | In copertina Ionogramma, particolare



# INDEX

<b>Abstract</b>	<b>7</b>
<b>Introduction</b>	<b>7</b>
<b>1. Radar types</b>	<b>10</b>
<b>2. Characteristics of the PRC ionosondes</b>	<b>12</b>
<b>3. Coherent radar signal processing</b>	<b>15</b>
<b>4. Transmitting stations</b>	<b>17</b>
<b>5. Receiving Stations</b>	<b>19</b>
<b>6. The data center</b>	<b>20</b>
<b>7. The Web site</b>	<b>20</b>
<b>8. Antennas</b>	<b>22</b>
<b>9. Conclusions and developments</b>	<b>24</b>
<b>Bibliography</b>	<b>24</b>
<b>Sitography</b>	<b>25</b>



## Abstract

IonoNet is an INGV multi-static cooperative radar network of Pseudo Random Code (PRC) ionosondes for oblique ionosphere soundings placed in different points of the national territory; in this way it will be possible to compare the ionosphere characteristics relating to points separated by approximately a few hundreds of km. The project has been funded within the “Piano Nazionale di Ripresa e Resilienza” PNRR of INGV “Meet” inside the activity 9.5 “*Design, realization and testing of ionosondes for oblique and vertical sounding, complete with data communication and remote access systems. Realization of the necessary software for the acquisition, pre-elaboration and automatic scaling of ionograms. Database of oblique and vertical ionograms, real-time electron density profiles and radio propagation parameters. Alert for disturbed ionospheric conditions.*” The project activities concern the design and construction of ionosondes for oblique and vertical soundings. The instruments will be comprehensive of systems for communication and analysis of the acquired data with the transformation of the oblique ionograms into vertical ones, for a better comparison with the observatories ionograms. The “autoscala” software will be used for the real-time generation of the electron density profiles and the calculation of all propagation parameters; based on the output of “autoscala”, ionospheric alerts will be generated, for civil and military uses, in case of disturbed conditions.

The oblique PRC ionosondes are constituted by two parts, a transmitting and a receiving ionosonde located in different places. The PRC ionosondes have been built using Software Defined Radio (SDR) devices that act as transmitter or receiver of the Radio Frequency (RF) signals. They generate all the signals necessary for the operation of the ionosondes such as the GPS signals acquisition used for time synchronization, the triggering of the RF power amplifier for long distance sounding, and the antennas switches. The SDR device is able to convert into an RF signal a pseudo random numerical sequence generated by a Personal Computer (PC) or receive and convert the RF antenna signals into a pseudo random numerical sequence on the PC; this is accomplished by means of a high speed Ethernet port (1Gb per seconds), used also to transmit the SDR data and configuration parameters. There is a wide choice of SDR configurations and a great versatility for these devices; with the possibility of changing frequencies and amplitude of transmitted waveform or applying filters in different bands. The receiving PRC ionosonde, placed at one of the ionospheric observatory, allows receiving and detecting at the same time the pseudo random coded signal transmitted contemporarily from different ionosondes, multiplying the observation possibilities of the ionosphere from different directions. It is possible to use the code with different random seed (used as station identifier parameter) at the transmitting ionosondes and using a precise time synchronization between transmitting and receiving ionosondes; the high precision is obtained using a GPS Disciplined Oscillator (GPSDO). The surveys will allow to map the ionosphere over large regions for the verification of theoretical models of the global ionosphere and local disturbed ionospheric conditions, and to investigate possible ionosphere- lithosphere coupling phenomena.

**Keywords** Oblique sounding; Ionosonde network; Software defined radio

---

## Introduction

IonoNet is a multi-static cooperative radar network of PRC ionosondes designed by INGV to map and study the ionosphere, its electron density profile and the radio propagation parameters. The



used ionosondes are bi-static radars that transmit an almost continuous wave. The network project aims to install four transmitting ionosondes sites in: Rome, Montelibretti (RM), Gibilmanna (PA), La Spezia and five receiving ionosonde in Rocca di Papa (RM), Preturo (AQ), Duronia (IS), Lampedusa (AG), Castello Tesino (TN) to cover a large part of our national territory from north to south (more details in Chapter 4 and 5). At present, not all planned sites have been activated yet: the transmitters at Gibilmanna and La Spezia, and the receiving stations at Castello Tesino and Lampedusa, are going to be activated in the next months. Most of the receiving sites are sites of the INGV Geomagnetic Observatories (CTS, DUR, LMP), chosen for opportunities as INGV infrastructure and after a compatibility test between ionosonde instrumentations (mainly a RF receiver) and geomagnetic magnetometers. The choice of the transmitting sites of Roma, Montelibretti and Gibilmanna has been made considering that the INGV ionospheric observatories are already equipped with antenna structures. On the other hand, smaller antennas have been developed for the receiver sites (see Chapter 9 about antennas).

To build a network of ionosondes, using multiple transmitting sites, there are two possible configurations: one is to use different time slots for each transmitter (transmitting at different times), the other is to transmit simultaneously with different codes in such a way to be recognized and discriminated by the receiving stations. The first method reduces the number of possible soundings, because of the waiting the four transmission times at each receiver; the second method can make four soundings at the same time at each receiver but with the drawback of a more complicated random coded transmission system. Moreover, the use of SDR (Software Designed Radio) devices helps to simplify complicated RF systems thanks to their programmability. SDRs are very adaptive devices that can be programmed by a software code written in Python or C++ and connected to a PC through a fast Ethernet line (RJ48) or USB, for configuration and data transmission.

A Classic ionosonde [Bibl, 1998] is a pulsed radar that, by emitting a sequence of radio frequency pulses and measuring the delay time between the transmitted pulse and the received one, makes it possible to obtain the distance of a “target”, i.e., a reflector, hit by the transmitted impulse, knowing the speed of propagation of the wave in the medium. By means of this technique it is possible to measure the height of the reflecting layers of the ionosphere [1] [Arokiasamy et al., 2002; Davies, 1990; McNamara, 1991]. In vertical surveys, the transmitter and receiver are placed in the same observation point. This causes a problem for the receiver during the transmission of the impulse, because it is directly hit by the transmitted high-power signal, which can create problems of saturation or even failure of the first stages of the receiver; therefore, it is turned off for the entire duration of the transmission impulse (“blind time”). In oblique surveys, since the transmitter and receiver are located in places separated by hundreds or thousands of kilometres, this problem does not arise; continuous wave (CW) radar can also be easily used [Farnett et al., 1990; Alter et al., 2008]. However, the technique, used over large distances, requires time synchronization of the transmitted and received signal for the exact determination of the arrival time of the echo. In this case, it is possible to use time synchronization techniques with GPS (Global Positioning System) systems, which allow synchronizing two devices located at a great distance with errors less than a microsecond. Moreover, through GPSDO (GPS *Disciplined Oscillator*) techniques it is possible to synchronize the phases of the signals of transmitter-to-receiver reference oscillators with very small phase errors. The evolution and miniaturization of electronic devices has also made it possible to create electronic components capable of operating at higher frequencies; this is especially true for digital electronic components. The creation of ever faster analog-to-digital converters (ADC) and digital-to-analog converters (DAC) (up to the order of GHz), with a large number of logic levels (24 bits), combined with the use of fast processors, have made it possible to replace most of the analog systems for radio frequency (RF) signals with digital devices. Finally, the introduction of programmable logics (e.g., *Programmable Logic Array* - PLA, *Complex Programmable Logic Device* - CPLD, *Field*



Programmable Gate Array - FPGA) has allowed for a considerable simplification in the design, construction and testing of even very complex systems. The 80s began with the introduction of DSP (*Digital Signal Processing*), real analog signal processors (mainly used in the audio field from 20 Hz to 20 kHz) which, by converting the analog signal into digital, processed it numerically with FFT (*Fast Fourier Transform*) techniques and then convert it back into an analog signal. Increasing the conversion speed and the transfer and processing speed has led to the processing of RF signals (from 100 kHz to 1 GHz). In this way, many of the difficulties inherent in analog RF electronics have been overcome, for example by solving the problems of coupling, noise and non-linearity of the various analog systems. The critical point remains that the RF signals, after conversion into numerical format, must transit through high-speed communication ports (an Ethernet port at 1 Gb/s has been used) towards the memories and processors. This speed is essential in these new systems because it limits the bandwidth, a fundamental characteristic of an ability of the device to faithfully reproduce a signal without generating distortions.

An example of how radio systems have been transformed following these innovations are the SDR devices [Rouphael, 2009] [2], which allow the creation of complex systems of modulation and demodulation of radio signals by writing few lines of program, considerably reducing the number of electronic circuits necessary for the treatment of analog signals and making it possible to implement telecommunications systems, RADAR, Bluetooth, Wi-Fi and more. The fact of being programmable allows, in a short time, to reconfigure the characteristics of the system by modifying operating frequencies, bandwidth etc., and the ability to implement improvements and updates, even remotely. There are a large number of SDR devices available on the market today with very varied characteristics. The use of commercial SDR devices in ionospheric radars is made possible both for the low frequencies tested (from 1 to 30 MHz) and for the little bandwidth required, as there are devices on the market that can work at frequencies thousands of times greater. Ordinary PCs connected via a fast Ethernet port can be used as digital signal processors (for example Ettus Research SDR), but there are also cheaper SDRs that use fast USB ports. These programmable devices applied to radar systems allow for considerable versatility; in fact, all the modulation and intermediate frequency (IF) oscillators are programmable, and the transmission and reception frequencies can be easily varied. Furthermore, the digital conversion techniques make it possible to program the signals generated and the used codes, allowing passing from a pulsed amplitude modulation radar to one with complementary phase coding simply by programming it with different data; finally, these techniques allow applying digital filters to the signals, which are less critical with respect to the realization of analog filters. With analogue techniques, these performances were almost impossible to achieve, or very expensive, it was necessary to create complicated systems with large banks of analogue filters for the different frequencies and for the different set of codes, not to mention that many of these filters over time, due to wear, lost their characteristics, compromising operation or forcing repeated calibrations.

The IonoNet project is based on the development of ionosondes for oblique surveys realized with SDR devices. This choice makes it possible to realize programmable instrument therefore versatile and innovative compared to classical ionosondes. The oblique ionosondes follow the AISP (Advanced Ionospheric Sounder Programmable) ionosonde [Zirizzotti et al., 2022] and CHIRP ionosonde [Zirizzotti et al., 2021] for vertical sounding completely designed and built at INGV laboratories using SDR devices but with the innovation of use a pseudo random sequence to code the transmitted CW signal.

The software to implement the Pseudo Random Code (PRC) on ionosonde devices has been already developed and shared on GitHub ([www.github.com](https://www.github.com), a hosting service for software projects). The software in the repository may be downloaded, cloned, modified, or otherwise used free of charge, in accordance with the GNU General Public License. In GitHub it is possible to find a huge quantity of projects for SDR devices, while complete implementations for PRC

ionosondes can be found at ionosondes Github site [4] of prof. Juha Vierine group with installation suggestions on Ubuntu operating system and instrumentation schemes. The shared Python software has been modified by us to extend the frequency range to 1-24.9 MHz, necessary to study the increased spectrum of frequencies that can be received when performing an oblique sounding, with a high frequency resolution of 0.1 MHz and a range resolution up to 1.5 km. The sounding duration time has been increased to 4 minutes with sounding starting at each hour at the minute 0 and ending at 56 for a total of 15 soundings every hour. The sounding for the 240 frequencies has a total duration of 4 minutes with 1 s for each sounded frequency. Considering the huge quantity of data produced by a receiving ionosonde, an automatic system of acquisition, communication and data storing and analysis has been developed together with an INGV internal web site [3] that will be published as an open site: [iononet.ingv.it](http://iononet.ingv.it), to show and download the acquired and analysed data.

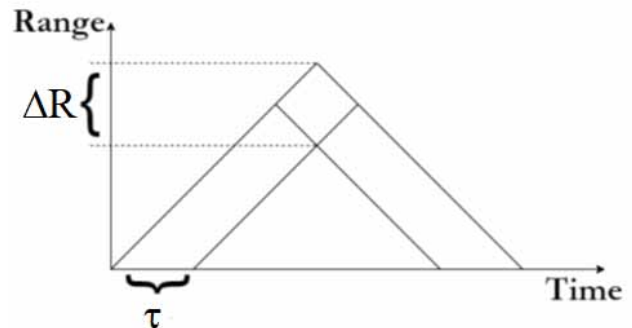
## 1. Radar types

To better understand the characteristics of the ionosondes that make the IonoNet, a brief summary of the various radar types, like pulsed, coded and chirp, is presented here [Arokiasamy et al., 2002; Farnett et al., 1990; Alter and Coleman, 2008; Zirizzotti et al., 2021; Zirizzotti et al., 2022].

The first classification is between the monostatic and bi-static radars. The first is characterised by a transmitter (Tx) and a receiver (Rx) that share the same antenna, while in the bi-static the Tx and the Rx are placed in different sites and use different antennas (there is also a third type: the multi-static radar, that uses many transmitters and many receivers, but it is not relevant in this work).

The simplest pulsed monostatic radar generates a RF pulse wave of short time duration ( $\tau$ ) (Figure 1). In this type of radar, the detection of an object (reflector) occurs at a range  $R = c t/2$ , that comes from the detection of the radar echo (a reflection of the transmitted pulse on the target) at a detection time  $t$  in a medium of wave speed  $c$  (air). Mathematically the detection of the target signal is done by a correlation calculation between the received signal and the transmitted waveform after a base band down conversion. The correlation result is a peak at the detection time  $t$ . The spatial resolution (“minimum distinguishable range”)  $\Delta R$  is directly related to the minimum pulse duration  $\tau$ . Therefore, the relation  $\Delta R = c \tau/2$  will allow to evaluate the minimum distinguishable distance between two nearby reflectors.

**Figure 1** Simple pulse representation in time-range domain.



The system is characterised also by a minimum detectable distance (called “blind range”). In fact, the receiver must be switched off during the transmission in order to avoid saturation or damage. As a consequence, in the simplest pulse radar the blind range is directly related to the pulse duration  $\tau$ , actually it is numerically equal to the resolution:  $R_{\min} = \Delta R$ .

For a better resolution and blind range, a very short pulse is necessary, but short pulses have less energy and larger bandwidth with respect to longer ones, compromising the target detectability. To resolve these problems a digital code can be added to the transmitted pulse dividing it in sub-pulses (Figure 2 and Figure 3).

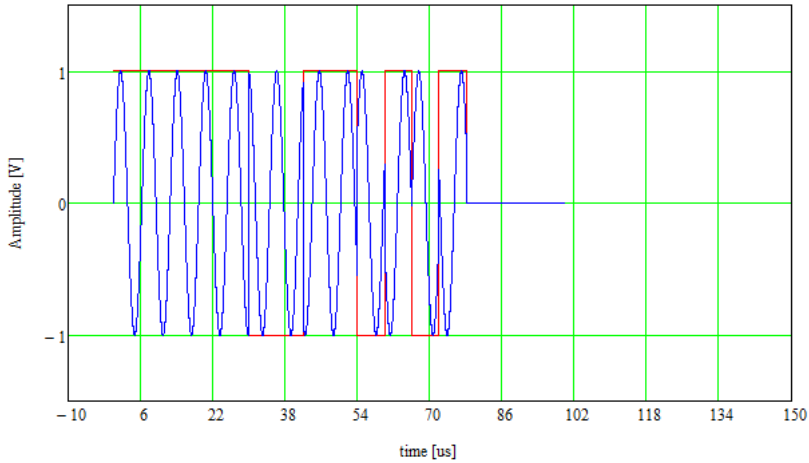


**Figure 2** Example of a 13 bit coded pulse (code:1 1 1 1 1 -1 -1 1 1 -1 1 -1 1).

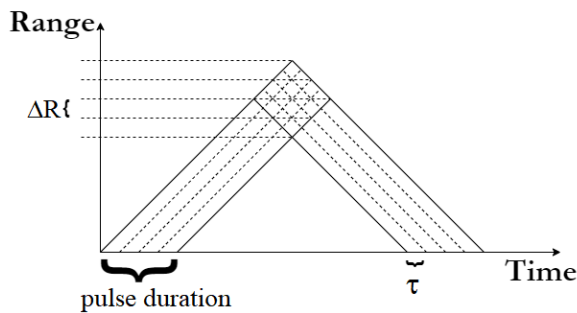


**Figure 3** Coded pulse representation in time-range domain.

In this phase-modulated coded radar the range resolution depends on sub-pulse duration ( $\tau$ ), while the total pulse duration can be stretched using long codes (with higher energy) to obtain a signal compression effect on the resultant correlation. The problem arising using such codes is the presence of “sidelobes”, located on the sides of the main reflected pulse, which makes the signal-to-noise ratio worse. Several types of code with different numerical sequences have been developed to obtain lower sidelobes with different code lengths (e.g., Barker codes [Farnett, 1990]).

There are other phase modulation schemes that uses more than two phase-offsets to divide the pulse, that are called poly-phase modulation schemes. Anyway, the complete sidelobes cancellation can be obtained using two or more complementary codes (Golay codes, Alter [2008]) that must be transmitted subsequently increasing the time needed for detection. The main advantage using a coded radar is the increased amplitude of the received target peak after the correlation process. The process is called “pulse compression” with the peak amplitude growing proportionally to the code length, which can be evaluated as a gain with respect to a simple pulse-radar.

The CW (Continuous Wave) radars are based on a different principle. The simplest CW radar transmitted signal is only a continuous RF wave, but in this elementary case, only the target speed can be detected, measuring the frequency shift of the received signal, due to the Doppler effect. This radar is commonly used in car speed measurements for traffic limitation. However, if the wave

is frequency modulated with a time dependent function (sweep) it is possible to measure the distance, indirectly, through a beat between the received and transmitted wave. In fact, the two waves are characterized by a different instantaneous frequency, due to time delay. Also in this case, a correlation between transmitted and received signals allows fast and precise target detections (a lot of information on this topic is available on Wikipedia pages about pulse compression [6]). The range resolution is (numerically) inversely proportional to the bandwidth of the transmitted signal: the larger the bandwidth (swept frequencies), the better the resolution obtained.

Moreover, ionosondes measure ionosphere layers' distances at different frequencies, this can be easily achieved also using a sort of "chirp radar": the carrier frequency varies continuously covering the entire band (1-15 MHz), but this band is divided into small intervals chosen to reach the required resolution (and ensuring that a single reflecting height is associated to a single interval). This method reaches similar performances to the sub pulse method of coded radar [Zirizzotti et al., 2021].

The new ionosonde for oblique soundings presented in this paper is basically a bi-static continuous wave radar.

## 2. Characteristics of the PRC ionosondes

The ionosonde for the oblique sounding that will be used in the IonoNet project is a coded continuous wave ionosonde, which utilizes long Pseudo-Random Coded transmit waveforms (PRC radar). The random code in the transmitted signal allows us to distinguish among signals transmitted from different sites of a multi-static cooperative radar network. A similar approach is used by the global positioning system (GPS) where a single GPS receiver can use the radar signals of several satellite at the same time, with the particularity that the transmitter start time is coded in the signals. PRC radars have several advantages: they can be used at low peak power, can measure range or velocity (using Doppler effect) over spread targets, they are relatively robust against external interference and they produce relatively low interference to other users that share the same portion of the electromagnetic spectrum. Moreover, the low cross correlation between coded signals from different transmitting stations allow to transmit, receive and elaborate the different received signals at the same time. This design is thus well suited for use in ionosonde networks [Floer, 2020].

The waveform generated by the PRC ionosonde is built on the base of a set of parameters included in the configuration files (\*.ini); in the following the parameter names will be enclosed in square brackets. We start from a sequence of random numbers that will define the phase values of the transmitted wave, after the formula:  $\varphi = \exp(j2\pi rnd)$ . The function *rnd* is a typical one that generates pseudo-random numbers, it is based on a seed specified by the parameter [*stationid*] that is equal to the code that identifies the transmitting station; in this way each receiving station is able to extract from the received signal only the sequence generated by the transmitter to be decoded. The sequence is made up by [*codelen*] values, this sequence might be longer than the one that will be actually transmitted, being this length fixed by the parameters [*pulselenght*] and [*ipp*] that specify the length of the pulse and of the transmission, respectively; this double specification was introduced to allow the possibility of transmitting a sequence of pulses or a continuous wave. If [*pulselenght*]<sup>3</sup> [*ipp*] only the first code values until [*ipp*] will be transmitted. If [*pulselenght*] < [*ipp*] after the first [*pulselenght*] values, the transmitted sequence goes on until [*ipp*] filling the values with zeroes (see Figure 4 where [*pulselenght*]=200 and [*ipp*]=400). When all the values till [*ipp*] are sent, the sequence starts again.

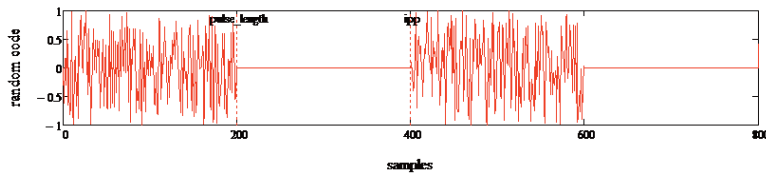


Figure 4 Coded pulse example in the case of pulsed signal.

The same result of putting  $[pulselenght] = [ipp]$  can be achieved by placing  $[pulselenght] = -1$ ; in this way the system recognizes that must send a continuous wave. There is a parameter  $[dec]$  that specifies an oversample, so that every value of the sequence is repeated  $[dec]$  times; therefore, the same value will be received  $[dec]$  times (plus noise) and averaged, increasing the signal-to-noise ratio. The parameter  $[samplerate]$  sets the sampling frequency, its reciprocal being the time interval between two samples; as a consequence, the value  $D = [ipp] \times [dec] / [samplerate]$  is the duration in seconds of the sequence of values actually to be transmitted. All the sequence is used to modulate a carrier at a single frequency, being its module equal to one and the phase calculated after the formula defined above. There is a last parameter  $[frequencyduration]$  that sets the transmission time at a single frequency. After the time  $[frequencyduration]$  expires, a new sequence is generated and transmitted using a different carrier frequency. Starting from 1 MHz, with 0.1 MHz steps, there are 240 different values, being the last one 24.9 MHz. The typical values used for the ionosonde parameters are:

$[codelen] = 10'000$

$[dec] = 10$ , so there are 100'000 total values

$[pulselenght] = -1$ , so a continuous wave is generated along D duration

$[samplerate] = 1$ , means 1 MHz, so the sample interval is 1  $\mu s$ , and  $D = 0.1 s$

$[frequencyduration] = 1s$ ;

therefore, the sequence is repeated 10 times at the same frequency before passing to the next frequency. The whole sounding lasts 4 minutes; it is repeated 15 times in an hour without breaks. The soundings start at minute 00 of each hour; to avoid loss of synchronisation between the transmitter and the receiver, GPSDO are used (with accuracy of about some nanoseconds). As said, the sounding duration takes 4 minutes, a duration comparable to that of the ionosondes currently working at the INGV. A lower duration with a shorter code would reduce the signal process gain useful in long distance connections with greater geometrical attenuations.

Some further considerations should be made about the bandwidth in view of the practical implementation of the system. We have just seen that the bandwidth occupied by the signal is what determines the distance resolution. Implementing a broadband radar presents difficulties if analog techniques are used, since all sections of the system have to work on broadband. Using modern SDR devices, the problem is simplified, and today devices are available that allow to easily obtain the desired bands for ionosonde applications (in addition to the device itself, it is to be taken into account the speed of the communication port used). For example, if you want to deal with a signal with a bandwidth of 200 kHz, you need to sample at least double the frequency. Generating a 200 kHz bandwidth analog signal with a D/A device and sampling to have at least 5 samples for each subpulse, an  $f_s$  (the sampling frequency) of 1 GHz is reached for a better condition. Assuming to have quantized integer data at 8 bits, a transfer speed of 8 Gbit/s (1 Gbyte/s) is reached; well, by now this speed is usual for an Ethernet or USB port.

Also in reception, the bandwidth occupied by the signal must be taken into account. Theoretically, the band occupied by a signal formed by a sequence of ideal pulses, obtained by sampling the received signal, is infinite, even if the spectrum from zero frequency up to  $f_s$  repeats itself identically at multiples of that frequency. If the sampling frequency is large enough than the quantity  $1/\tau$  (where  $\tau$  is the duration of the sub-pulse), and since the sampling process is not

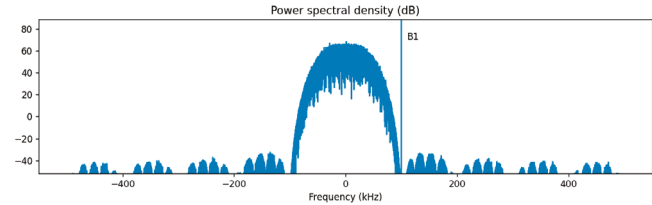
ideal, in practice the bandwidth is finite and, on the contrary, the energy tends to concentrate in a relatively small range around zero frequency. The following empirical formula allows evaluating the bandwidth occupied by a coded pulse signal (it does not depend on the code used):

$$B_4 = \frac{4}{\tau} \quad (2.1)$$

Figure 5 shows the power spectrum for a unitary random code signal of 100'000 samples used in the PRC ionosondes. The sub-pulse band  $B = fs/dec = 1/\tau = 100$  kHz ( $\tau = dec/fs = 10 \mu s$ , 10 samples @ 1 MHz); while with the previous formula it is calculated that  $B_4 = 400$  kHz; it can be calculated that 99% of the signal power falls within the  $B_1 = 100$  kHz band, as shown in our case in Figure 5. In this way, we can obtain the relation between the range resolution and bandwidth of the radar:

$$\Delta R = \frac{c \tau}{2} = \frac{c}{2 B_1} \quad (2.2)$$

Figure 5 Power spectrum of the random coded signal.



For a transmitted pulse with a 100 kHz bandwidth, the range resolution would be 1.5 km. In this case, the width of each sub-pulse is  $10 \mu s$ . By means of a low-pass filter, it is therefore possible to limit the band to a value like this without fear of distorting the signal and thus losing the possibility of detection. Then it is possible to proceed to choose a higher sampling frequency, so as not to run into aliasing problems.

In order to separate the ranges of the different sub-pulses when receiving a pulse-compressed signal, a deconvolution of the received radar signal is necessary. In fact, in order to determine the distance of the ionospheric layers, the echo is to be convoluted with the transmitted signal. To detect targets in the receiver signal, a matched filter is commonly used. This method is optimal when a known signal is to be detected among additive noise having a normal distribution. In a matched filter of impulse response function  $h(t)$  the output  $m(t)$  is the convolution of  $h(t)$  with the received signal  $E(t)$ :

$$m(t) = \int_0^t h(\tau) E(t - \tau) d\tau \quad (2.3)$$

The filter is matched to the transmitted waveform if the filter is built with its response function equal to the complex conjugate of the transmitted waveform  $Tx(t)$ :

$$m(t) = \int_0^t Tx^*(\tau) E(t - \tau) d\tau \quad (2.4)$$

The result of the integral (2.4) is equal to the correlation of the received signal and the transmitted waveform. But our signal is the result of a coding with a pseudo-random sequence, so it has ideally the same spectrum of a white noise; therefore, when receiving a waveform equal to the transmitted code, the (2.4) represents the autocorrelation of a white noise. From the signal theory the peak of autocorrelation of a white noise is equal to the variance ( $R_{xx}(0) = \sigma^2$ ).



In the case of uniform random distribution of values between  $a = -1$  to  $b = 1$ , we have  $\sigma^2 = (b-a)^2/12 = 0.333$  [Proakis and Manolakis, 1996] [7]. On the other hand, the sidelobes generated during the correlation process represent another kind of noise (an “error noise”), their maximum value is about  $\frac{b-a}{2\sqrt{N}}$ , that in our case ( $N = 10000$  is the “*codelen*” parameter) is equal to 0.01. So the SNR (Signal to Noise Ratio) is the ratio between the signal power and the square of the sidelobe amplitude  $SNR = \frac{N}{9} \approx 1111$  (30 dB, a better simulation in the next Chapter). In the PRC radar, the signal to noise ratio is proportional to numbers of pseudo random samples.

### 3. Coherent radar signal processing

In the IonoNet ionosondes, the receiver hardware is minimal, the matched filter at the receiver output is not present, and its function is accomplished by software. Following a down conversion in base band, the acquired signal is directly saved in a data file. After data acquisition, the signal analysis starts in a separate process, and each signal received from the various transmitters is processed separately.

In the signal processing, the correlation operation between the transmitted signal and the echo signals is necessary to separate the ranges measurements of the different pulses when receiving a pulse-compressed signal. In order to estimate the echo as a function of range, the transmitted signal needs to be deconvolved, this can be performed either in the frequency domain or in the time domain; in radar literature slight different methodologies are reported, such as matched filter or inverse filtering to denote these operations. An equivalent and more general method can be used from linear regression of Kaipio [2010] that differs from standard practice methods used in radar literature. Here in following the technique of linear least-squares will be utilized, similar to Floer [2020]. The measured radar signal is a convolution between the transmitted signal and the echo for each range. The received signal can be expressed as the sum of the received sub-pulses, where each received sub-pulse is a product of the delayed transmitted pulse  $E_{tr}$  and a scattered signal amplitude  $V_{tr}$  from the target in the interval  $r$  of instant  $t$  as shown in the time-range representation diagram in Figure 6. We can express generally the received signal as a convolution:

$$m(t) = \int_0^t E(t - \tau)V(\tau)d\tau \quad (3.1)$$

and using sampled signals we can write:

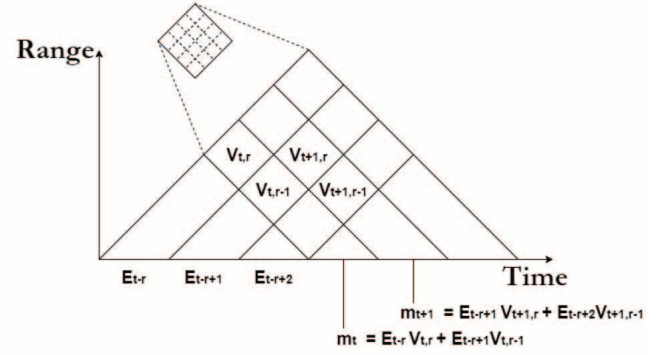
$$m_t = \sum_r^R E_{t-r} V_{t,r} + n_t \quad (3.2)$$

The received radar signal  $m_t$  is a vector where each element is given by the product between the transmitted pulse  $E$  and the amplitude of the scattered signal  $V$  at time  $t$  and the corresponding range  $r$ . The last term  $n_t$  represents the ambient noise. We assume that the scattered signal amplitude remains constant throughout the period  $T_c$  in which the pulse propagates through the scattering volume (coherent ionosphere); we can exclude the dependence of  $V$  from  $t$  and re-write the received signal as:

$$m_t = \sum_r^R E_{t-r} V_r + n_t \quad (3.3)$$



**Figure 6** Range-time diagram for a pulse compressed signal representation. The sub-pulses within the transmit pulse are denoted  $E$ , while the scattering signal is denoted  $V$ .



Where  $V$  now only is a function of range  $r$ . Radar targets that have a constant scattering amplitude over a pulse period  $T_c$  is by convention considered as a “coherent” target. Radar systems that rely on this constant scattering amplitude are thus referred to as coherent radars. When the time dependence of the scattered amplitude  $V$  is removed, the equation (3.3) becomes a convolution equation. In the case of ionosonde measurements we can typically make this assumption.

The validity of the assumption that the scattered amplitude is constant throughout the long pulse-period  $T_c$  depends on the Doppler width of the scattered spectrum. If the scattered signal has a broad Doppler width it means that the scattering medium changes rapidly relative to the duration of the pulse and the target is deemed “incoherent”. Considering the time interval  $T_c = L/fs$  of coherence over  $L$  samples, considering the index  $i \in [iL \dots (i+1)L - 1]$  on the coherent interval, the vector  $[V_{0,i} \dots V_{R,i}]^T$  radar echoes for each transmitter we can write the received data vector  $m_i = [m_{iL}, m_{iL+1}, \dots, m_{(i+1)L-1}]^T$  as:

$$m_i = A_i v_i + n_i \quad (3.4)$$

Where:

$$A_i = \begin{bmatrix} E_{iL} & E_{iL-1} & \dots & E_{iL-R} \\ E_{iL+1} & E_{iL+1-1} & \dots & E_{iL+1-R} \\ \vdots & \vdots & \ddots & \vdots \\ E_{(i+1)L-1} & E_{(i+1)L-1-1} & \dots & E_{(i+1)L-1-R} \end{bmatrix} \quad (3.5)$$

Thus, the convolution operation (eq. 3.3) can be constructed as a matrix multiplication, where the inputs is converted into a Toeplitz matrix (diagonal-constant matrix), and thanks also to the linearity of the correlation equation, the representation of the received signal can be done in the form of matrices:

$$m = Av + n \quad (3.6)$$

where the Toeplitz matrix  $A$  relates the transmit signal and the constant scattered signal  $v$  [Vierinen et al., 2016]. Because the scattered signal is assumed constant over the pulse-duration, the linear-least-squares method can be used for obtaining an estimation of the scattered signal  $v$ :

$$v = (A^H A)^{-1} A^H m \quad (3.7)$$

It is important to notice that this analysis is more general and works for any kind of transmitted waveforms. For a comparison between simple correlation and linear regression method, a mathematical simulation has been done to calculate amplitude and signal to noise ratio of PRC radars signals with different pulse lengths. In Table 1 the results of the simulation are shown.

ipp	len	Linear regression			Correlation		
		Peak Amp.	Noise	SNR (dB)	Peak Amp.	Noise	SNR (dB)
400	200	0,51	0,037	22,6	0,09	0,007	22,8
400	300	0,67	0,028	27,6	0,17	0,008	27,7
400	400	0,99	0,004	47,6	0,33	0,012	29,1
500	200	0,52	0,036	23,2	0,07	0,006	21,5
500	300	0,66	0,033	26,1	0,13	0,007	25,3
500	400	0,75	0,028	28,7	0,20	0,008	27,4
500	500	0,99	0,004	47,6	0,33	0,012	29,1

**Table 1** Comparison between different elaboration processes.

The linear regression method shows better SNR values in the cases of continues waveforms (ipp=len parameter) due to the fact that with this method the whole bi-dimensional measured values are used, while with the correlation only a single trace of measures is used. The *len* values have great weight in the peak amplitude calculation in both processes.

## 4. Transmitting stations

Four transmission sites were defined in the project: Rome, Montelibretti (RM), La Spezia and Gibilmanna (PA), (Figure 7).



**Figure 7** Map of Tx and Rx ionospheric station and their distances.

All the selected sites are located at one of the INGV locations, except the Montelibretti site, which is at the CNR (Consiglio Nazionale delle Ricerche) research centre that hosts our instrumentations thanks to a memorandum of understanding wrote between the two national research institutions. This site is very near to Rome and was chosen in order to ensure a transmitting site in central Italy in case the Rome site should become unavailable for the “IonoNet” instrumentation.

The software of the transmitting stations consists of a Python code for the operation of the SDR device of the ionosondes. The software used for the stations is a modified version of the software available on the Vierinen ionosonde GitHub site [4].

The software uses the Python UHD library and must be installed by compiling the library directly on the computer. The transmitting Python process “*tx\_uhd.py*” is launched by the batch file “*start\_tx.sh*” (the file starts automatically as the computer is switched on). The process runs

continuously, transmitting every four minutes starting from the minute 0; it takes 4 minutes to sweep all the frequencies from 1 to 24.9 MHz defined in the configuration file “*config/station\_name.ini*”. The configuration file has the same format for receiving and transmitting stations with the main configuration parameters of the station. An important transmitting parameter is the “*station\_id*” because it is the seed of the random data and is essential for the station recognition. In the Table 2 the list of station ID parameters of the working transmitting stations is reported.

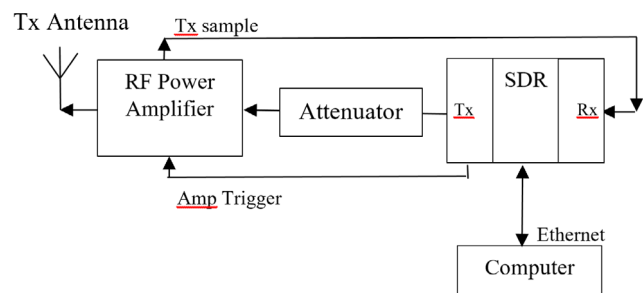
Transmitting station	ID	Note
Roma	1	transmitting
Montelibretti (RM)	10	transmitting
La Spezia	20	working in progress
Gibilmanna (PA)	30	working in progress

Table 2 Transmitting stations IDs.

Other important parameters are the “*transmit\_amplitude*” (0.33 default value to have a 0 dBm output voltage), “*tx\_addr*” and “*rx\_addr*” (example of SDR address: 192.168.10.2) Ethernet addresses of the SDR, “*instrument\_name*” for the station name.

The Python code starts with the configuration of the device. The time synchronization process uses the GPSDO on board of the SDR device. The code searches and locks the GPS satellites; it waits 30s checking if the connections to the GPS satellites are stable. Following the synchronization stage, the code waits for the next slot to start the transmissions, starting from 0 at step of 4 minutes. At the Roma and Gibilmanna stations due to the fact that there are other two vertical ionosondes (AIS and Lowell Digisonde) the slots are reduced to minutes 0-10, 14-25, 29-40, 44- 55. It is important to note that all transmitters are synchronised, so they start to transmit at the same time, with the same settings (from 1 to 24.9 MHz with steps of 0.1 MHz and duration of 1 second for each frequency), but using different codes, generated by the station ID random seeds.

Figure 8 Transmitting station block diagram.



In Figure 8 there is a sketch of the instrumentation connection of the oblique ionosonde. The computer in a minimal station configuration is an NVIDIA Jetson Nano single card computer with the Ubuntu operating system. The Power RF amplifier is a Tomco B500, a 500 W continuous wave amplifier. The variable attenuator is used to improve the matching. The antenna system is discussed in a following Chapter. The SDR generates the Amp Trigger signal through the GPIO programmable lines and reads the TX sample signal to measure and check the presence of the RF transmitted signal. The GPIO 3.3V level is shifted to 5V of the power amplifier trigger using the circuits in Figure 9 directly connected to the SDR receiver daughterboard.

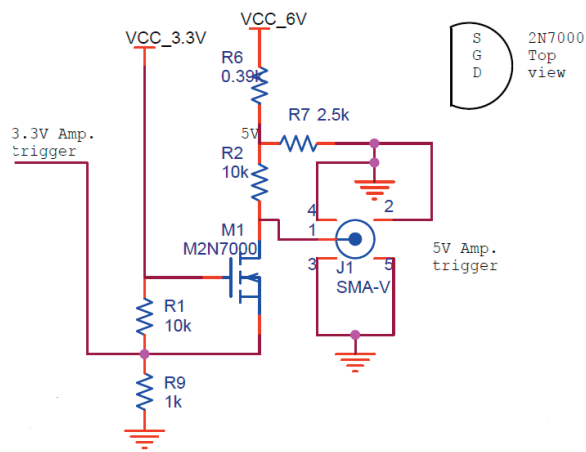


Figure 9 Level shifter circuit for the amplifier trigger.

## 5. Receiving Stations

It was decided to use the sites of the geomagnetic observatories of the INGV to host the receiving stations: Preturo (AQ), Duronia (CB), Lampedusa (AG), Castello Tesino (TN) as they have the infrastructures suitable for the installations after a check to ensure that the receiving station does not disturb the measurements of geomagnetic field. Rocca di Papa (RM) was added to these stations being close to the Rome INGV site and allowing a near-vertical ionogram, comparable with the ionograms carried out at the ionospheric observatory of Rome.

In Figure 10 a sketch of the receiving station is showed. The antenna is an MFJ-1886, a broad band receiving loop antenna, it works from 500 kHz to 30 MHz with quite good performance.

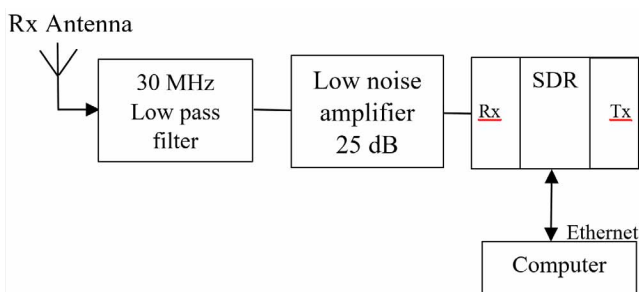


Figure 10 The receiving station block diagram.

The antenna has an internal amplifier connected directly on the antenna loop to reduce the cable noise. The antenna cable powers the amplifier via a bias tee and at the end of the cable a Mini Circuits low pass filter SLP30 is connected to a low noise Mini Circuits amplifier ZX60100VHX with 35 dB gain. The amplifier is connected directly to the receiver daughter board LFRX of N210 Ettus Research SDR. The acquisition computer is an i7 processor and 8 GB of RAM memory.

In the computer, the receiving process `rx_uhd.py` starts in the batch file `start_rx.sh`, the process run continuously every four minutes starting from 0 minute, sweeping all the frequencies defined in the configuration file `config/station_name.ini` and synchronised with the transmitting slots at steps of 4 minutes.

The demodulated received data are saved in a RAM disk for a faster data processing, the RAM directory `/dev/shm` (`data_dir`) is defined in the configuration files. The saved data files are binary files (es: `raw-XXXXX.bin`) where the Xs are the Unix time stamps of the ionospheric sounds for each sounded frequency. After the receiving process, the data analysis Python program `analyze_ionograms.py` elaborates the received binary files and starts automatically and

continuously at the end of the acquisition process. Different analysis programs start, one for each transmitter with different station ID (different random seed). The synchronization with the acquisition and the list of stations to analyse is wrote in the batch file "*start\_an.sh*". The system can be configured to start up automatically at the system booting. The output of the analysis process is stored in the "results" directory for Rome transmitter and "resultMTB" for Montelibretti transmitter. These folders have sub-folders named with year, month, day, and hour. For each sounding two files are stored in the hour directory: the ionogram PNG picture file named "*year-month-dayThour-minute-seconds.png*" and the binary data file of the inogram in "HDF5" Hierarchical Data Format [5] and named "*ionogramm-year-month-dayThour-minute-seconds.h5*". At the end of the analysis process, the binary files are deleted to avoid filling the data disk. For each hour at the receiving station an amount of 22 MBs are produced in 30 files (192 GB/year). In the receiving computer, an FTP server is running to allow the files download and TeamViewer server for the remote controls of the station.

## 6. The data center

All the files produced at the different receiving stations are saved in the datacentre at Rome INGV headquarter. The data files (\*.png pictures and h5 binary files) are downloaded automatically using the ftp protocol by an analysis and download computer named IONO-CALC. The downloads are programmed every 4 minutes in the "*utilità di pianificazione*" running a "*scaricami2.py*" python program that performs all the files downloads from the Receiving stations. The files are stored in a Synology NAS (Network Attached Storage) named "IonoNet" connected to the internal network of the INGV. The main IonoNet data directory of the acquired ionograms is named "*Ionogrammi*"; inside it there are the directory of receiving stations ("*Aquila*", "*Duronia*", "*Rocca*"), inside each of them there is the transmitting station ("*Roma*", "*Montelibretti*") and finally the same structure of the receiving disk with year, month, day and hour.

After midnight, every day the computer runs a couple of batch files for data analysis from the "*Documenti*" directory:

- lono\_elab.bat: it transforms the h5 oblique ionogram file in vertical ionogram RDF data format (following the Martyn theorem [Martyn, 1935]) and it runs the Autoscala program [Scotto, 2002; Pezzopane, 2007] to scale the vertical ionogram;
- lono\_overview: it creates an overview and reports of the elaboration.

The elaborated files are stored in the "*Verticali*" directory with the same structure of the ionogram-directory with the "*output*" directory added in the hour directory containing all the scaled ionograms and files.

## 7. The Web site

The Synology NAS has the possibility to host web server. To show, control and download the acquired data a web site has been developed at the address "[iononet.int.ingv.it/joomla](http://iononet.int.ingv.it/joomla)" using the Joomla Content Management System (CMS). In the web site it is possible to get updated information on measures, instrumentations, stations and plots.

The vertical ionogram are stored in the data centre in RDF file format allowing to run the Autoscala program to scale the ionograms and calculate all the ionogramm parameters. The plots of the foF2 parameters are shown on the site compared to the geomagnetic horizontal components obtained from the geomagnetic observatory of L'Aquila as shown in Figure 13. The horizontal component of the geomagnetic field is useful to highlight the magnetic storms



and in the plots the effects on the foF2 parameters due to the magnetic storms are visible (negative ionospheric phases). In Figure 13, the “clouds” of points visible in some parts of the plots are due to a not perfect calibration of the autoscaling program (they correspond to times when the foF2 is not well determined, the program is to be improved at a later stage).

On the WEB site the ionograms are divided in two categories: acquired and processed ionograms. The acquired ionograms are shown without changes as they are acquired by the ionosondes and plot in colour maps as shown in the Figure 11. In the data process the oblique ionogram are transformed in vertical ionograms centred in the middle point of the line that link the two stations (Figure 12).

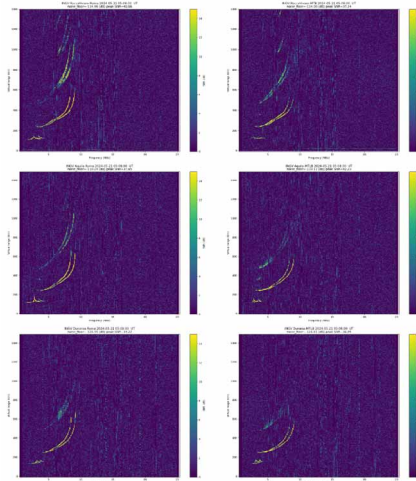


**Figure 11** Comparison between the acquired ionogram as shown on the website.

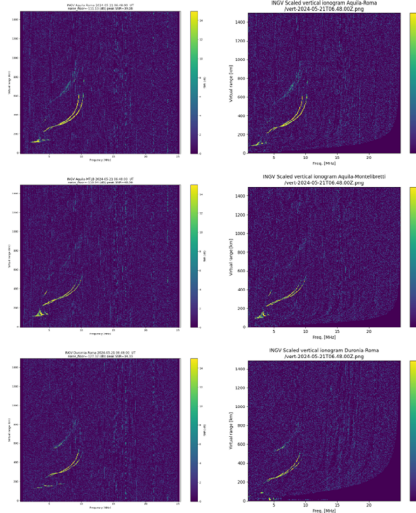


**Figure 12** Comparison between oblique and vertical ionograms.

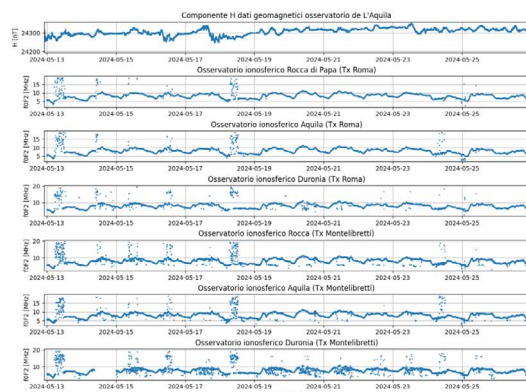


**Figure 13** foF2 plots compared with the geomagnetic H component.

The development of the data elaborations is in progress to obtain better results. Nowadays the IonoNet site is visible only internally from INGV network, a new datacentre and web site will be built to improve the service offered and to show the results to a wide public.

## 8. Antennas

The antenna system present in the Rome ionospheric observatory uses 2 side-by-side pairs of antennas, orthogonal to each other. The basic antenna is a progressive wave antenna of the “delta” type [Gilli, 2018]. Figure 14 shows the mechanical characteristics of a single antenna. Ionosondes at ionospheric observatories usually use two antennas, one for transmission and one for reception, orthogonal to each other. Figure 15 shows the cumulative measured gain of both (the small losses due to the imperfect impedance matching between antennas and cables have also been included). The indicated values refer to the maximum radiation, oriented towards the vertical.

Figure 14 Physical-mechanical characteristics of the “delta” antenna used for transmitting.

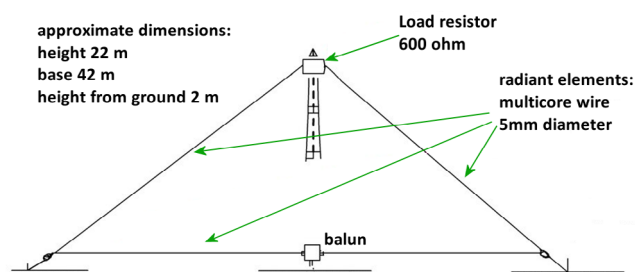
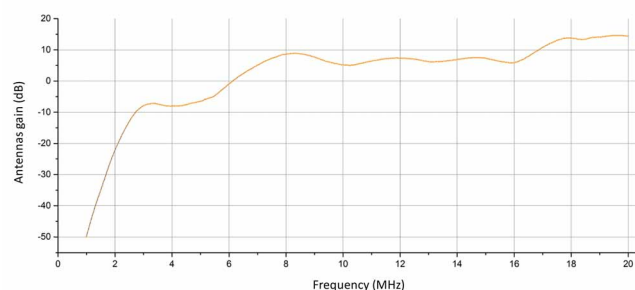


Figure 15 “Delta” antennas gain.



The transmitting station at Montelibretti makes use of a new antenna system, designed at INGV both for vertical sounding and oblique purposes (limited to near-to-vertical). The standard antenna system of an ionospheric observatory (like the one in Rome) makes use of very tall poles, so a different solution, based on shorter poles, was investigated; it implies a loss of efficiency, but the system becomes easier to install.

By means of dedicated software, the behaviour of many wire configurations was simulated (to forecast the gain and the *Voltage Standing Wave Ratio* - VSWR), all based on the “progressive wave” principle; this is necessary for a good performance over the wide frequency interval to be scanned. Among many types of antennas: 1) an “upside-down” delta (with the vertex pointing downward), 2) a bending delta (its plane is not vertical but inclined), 3) a “butterfly” (the wires form two triangles with a common vertex, they are put on a vertical plan; sometimes it is used by the radio hams), 4) a delta with an extended base plane (in the standard delta there is only a wire at the triangle base, in this case there are four conductors that form a horizontal square, with the original wire forming the diagonal).



Starting from the typical 600 ohm (pure) resistive load placed in the vertex, many different solutions have been simulated: different resistive values, values with complex impedance (with inductive or capacitive reactance); also different placement of the load have been simulated, e.g. feeding the antenna on the top vertex and putting two loads in the bottom vertexes toward ground (without the base wire).

Eventually, a solution was adopted that, though not optimal, is very simple because it follows the “delta” antenna design principle, with a 600 ohm load on the vertex. It adopts a pole that is as high as possible without the need of a special base of the pole (difficult to build). Once this constraint was set, the simulation results suggested that the longer the wires, the better the efficiency, so the longest base wire was chosen (suitable with the room available on the site). The result is an antenna with a shape similar to the one shown in Figure 14, but the pole is only 12 m high, while the base wire is at 2 m above the ground and is 45 m long.

The gain of this antenna varies, in the band 2-22 MHz, between -13 and +3.3 dBi, and the radiation diagram shows its maximum toward the zenith (if this is not the case, the gain value toward the vertical was calculated anyway). The lower gains occur at lower frequencies, a typical feature of this kind of antennas; unfortunately, the performance worsens further because the height has been lowered, which deteriorates the performance more at the lower than at the higher frequencies. Anyway, it can be noted that the -13 dBi value occurs only at 2 MHz, while considering the 3 MHz gain, it increases to -5.2 dBi. All these values are considered acceptable. The VSWR varies between 1.3 and 2.6; in this case the variations occur along all the scanned band (1-30 MHz), having many maxima and minima; however, the losses due to the mismatches remain within acceptable limits. Lastly, since the radiation pattern is rather wide, even though most of the energy is radiated toward the vertical, oblique soundings are allowed if the ray path forms with the vertical an angle less than about 30°.

The receiver loop antenna is the MFJ-1886 produced by MFJ Enterprises Inc., shown in Figure 16. The MFJ-1886 is an amplified antenna with a balanced-input low noise preamplifier working between 0.5 and 30 MHz. The used device is the Mini-Circuits monolithic GALI-74. In Figure 17 the top view of the radiation pattern is shown, important to notice that the maximum sensibility of the antenna is along the antenna radius while its sensibility is null in the front area.



Figure 16 MFJ-1886 loop antenna.

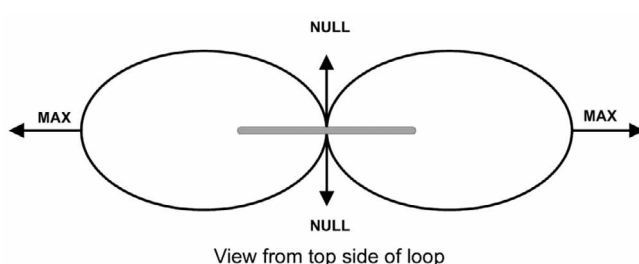


Figure 17 Radiation diagram of the MFJ-1886 antenna.

## 9. Conclusions and developments

With this report, we have intended to describe the work done to set up a national network of ionosondes for oblique soundings, in order to provide the technical information for allowing the reproducibility of the results. Another aim is to increase the interests of the entire scientific community in these type of measurements, promoting the establishment of a space weather service. The initial effort performed by the INGV to set up such a network has been great, but the greatest effort will be in its maintenance. That effort will be compensated by a deep and detailed analysis of the data acquired for the development of a better comprehension of the local variations in the ionosphere. There is also the possibility to relate these variations to ionosphere-lithosphere coupling phenomena [Ippolito, 2020; Perrone, 2018].

## Bibliography

- Alter J.J., and Coleman J.O., (2008). *Digital Signal Processing*. Chapter 25 of "Radar Handbook, 3<sup>rd</sup> edition", Skolnik M. I., McGraw Hill.
- Arokiasamy B.J., Bianchi C., Sciacca U., Tutone G., and Zuccheretti E., (2002). *The new AIS-INGV ionosonde design report*. Rapp. Tec. INGV, 12.
- Bibl K., (1998). *Evolution of ionosondes*. Annali di Geofisica, vol.41, n.5-6.
- Davies K., (1990). *Ionospheric radio*. P. Peregrinus London.
- Farnett E.C., Stevens G.H., (1990). *Pulse Compression Radar*, Chapter 10 of "Radar Handbook, 2nd Ed.", ed. Skolnik M., McGraw Hill.
- Floer M., (2020). *Design and Implementation of a Software Defined Ionosonde. A contribution to the development of distributed arrays of small instruments*. Master thesis; 2020-06-29, UiT The Arctic University of Norway, <https://munin.uit.no/handle/10037/19423>
- Gilli L., Sciacca U., and Zuccheretti E., (2018). *Calibrating an Ionosonde for Ionospheric Attenuation Measurements*. Sensors, 18(5), 1564; <https://doi.org/10.3390/s18051564>
- Ippolito A., Perrone L., De Santis A., Sabbagh D., (2020). *Ionosonde data analysis in relation to the 2016 central Italian earthquakes*. Geosciences, 10(9), 354, <https://doi.org/10.3390/geosciences10090354>
- Kaipio J., Somersalo E., (2010). *Statistical and Computational Inverse Problems*. Springer. ISBN 10: 1441919643.
- Martyn D.F., (1935). *The propagation of medium radio waves in the ionosphere*. Proc. Phys. Soc., 47, 323.
- Mc Namara, L.F., (1991). *The Ionosphere: Communications, Surveillance, and Direction Finding*. Krieger Pub. Co.
- Perrone L., De Santis A., Abbattista C., Alfonsi L. et al., (2018). *Ionospheric anomalies detected by ionosonde and possibly related to crustal earthquakes in Greece*. Annales Geophysicae, Volume 36, Number 1, 2018, pp. 361-371(11), <https://doi.org/10.5194/angeo-36-361-2018>
- Pezzopane M., and Scotto C., (2007). *Automatic scaling of critical frequency foF2 and MUF(3000)F2: A comparison between Autoscala and ARTIST 4.5 on Rome data*. RADIO SCIENCE, VOL. 42, RS4003, <https://doi.org/10.1029/2006RS003581>
- Proakis J.G., and Manolakis D., (1996). *Digital Signal Processing: Principles, Algorithms, and Applications*. Prentice-Hall, INC. ISBN 0-13-394338-9
- Rouphael T.J., (2009). *RF and Digital Signal Processing for Software-Defined Radio - A Multi-Standard Multi-Mode Approach*. British Library Cataloguing-in-Publication Data.
- Scotto C., and Pezzopane M., (2002). *A software for automatic scaling of foF2 and MUF(3000)F2 from ionograms*. Proceedings of URSI 2002, Maastricht, 17 – 24 August, Int. Union of Radio Sci., Ghent, Belgium.

- Vierinen J., Chau J.L., Pfeffer N., Clahsen M., and Stober G., (2016). *Coded continuous wave meteor radar*. Atmos. Meas. Tech., 9, 829-839, <https://doi:10.5194/amt-9-829-2016>
- Zirizzotti A., Bagiacchi P., Baskaradas J.A., Sciacca U., and Zuccheretti E., (2021). *Ionosonda SDR per sondaggi obliqui*. Rapp. Tec. INGV, 431: 1-32 (in Italian). <https://doi.org/10.13127/rpt/431>
- Zirizzotti A., Sciacca U., Zuccheretti E., and Baskaradas J.A., (2022). *AISP ionosonda programmabile*. Rapp. Tec. INGV, 458: 1-32 (in Italian). <https://doi.org/10.13127/rpt/458>

## Sitography

- [1] Australian Space Weather Forecasting Center. Introduction to HF radio propagation.  
<https://www.sws.bom.gov.au/Educational/5/2/2>
- [2] Ettus Research - <https://www.ettus.com/product-categories/usrp-networked-series/>
- [3] IonoNet project site: <http://iononet.int.ingv.it/joomla>
- [4] Vierinen J., Floer M., Mikko Syrjäsoo, Peje Nilsson. Github Ionosonde software repository:  
<https://github.com/jvierine/ionosonde>
- [5] Wikipedia page on Hierarchical Data Format:  
[https://en.wikipedia.org/wiki/Hierarchical\\_Data\\_Format](https://en.wikipedia.org/wiki/Hierarchical_Data_Format)
- [6] Wikipedia page on pulse compression: [https://en.wikipedia.org/wiki/Pulse\\_compression](https://en.wikipedia.org/wiki/Pulse_compression)
- [7] Wikipedia page on uniform distribution:  
[https://en.wikipedia.org/wiki/Continuous\\_uniform\\_distribution](https://en.wikipedia.org/wiki/Continuous_uniform_distribution)

# QUADERNI di GEOFISICA

ISSN 1590-2595

<https://istituto.ingv.it/it/le-collane-editoriali-ingv/quaderni-di-geofisica.html/>

I QUADERNI DI GEOFISICA (QUAD. GEOFIS.) accolgono lavori, sia in italiano che in inglese, che diano particolare risalto alla pubblicazione di dati, misure, osservazioni e loro elaborazioni anche preliminari che necessitano di rapida diffusione nella comunità scientifica nazionale ed internazionale. Per questo scopo la pubblicazione on-line è particolarmente utile e fornisce accesso immediato a tutti i possibili utenti. Un Editorial Board multidisciplinare ed un accurato processo di peer-review garantiscono i requisiti di qualità per la pubblicazione dei contributi. I QUADERNI DI GEOFISICA sono presenti in "Emerging Sources Citation Index" di Clarivate Analytics, e in "Open Access Journals" di Scopus.

QUADERNI DI GEOFISICA (QUAD. GEOFIS.) welcome contributions, in Italian and/or in English, with special emphasis on preliminary elaborations of data, measures, and observations that need rapid and widespread diffusion in the scientific community. The on-line publication is particularly useful for this purpose, and a multidisciplinary Editorial Board with an accurate peer-review process provides the quality standard for the publication of the manuscripts. QUADERNI DI GEOFISICA are present in "Emerging Sources Citation Index" of Clarivate Analytics, and in "Open Access Journals" of Scopus.

# RAPPORTI TECNICI INGV

ISSN 2039-7941

<https://istituto.ingv.it/it/le-collane-editoriali-ingv/rapporti-tecnici-ingv.html/>

I RAPPORTI TECNICI INGV (RAPP. TEC. INGV) pubblicano contributi, sia in italiano che in inglese, di tipo tecnologico come manuali, software, applicazioni ed innovazioni di strumentazioni, tecniche di raccolta dati di rilevante interesse tecnico-scientifico. I RAPPORTI TECNICI INGV sono pubblicati esclusivamente on-line per garantire agli autori rapidità di diffusione e agli utenti accesso immediato ai dati pubblicati. Un Editorial Board multidisciplinare ed un accurato processo di peer-review garantiscono i requisiti di qualità per la pubblicazione dei contributi.

RAPPORTI TECNICI INGV (RAPP. TEC. INGV) publish technological contributions (in Italian and/or in English) such as manuals, software, applications and implementations of instruments, and techniques of data collection. RAPPORTI TECNICI INGV are published online to guarantee celerity of diffusion and a prompt access to published data. A multidisciplinary Editorial Board and an accurate peer-review process provide the quality standard for the publication of the contributions.

# MISCELLANEA INGV

ISSN 2039-6651

[https://istituto.ingv.it/it/le-collane-editoriali-ingv/miscellanea-ingv.html](https://istituto.ingv.it/it/le-collane-editoriali-ingv/miscellanea-ingv.html/)

MISCELLANEA INGV (MISC. INGV) favorisce la pubblicazione di contributi scientifici riguardanti le attività svolte dall'INGV. In particolare, MISCELLANEA INGV raccoglie reports di progetti scientifici, proceedings di convegni, manuali, monografie di rilevante interesse, raccolte di articoli, ecc. La pubblicazione è esclusivamente on-line, completamente gratuita e garantisce tempi rapidi e grande diffusione sul web. L'Editorial Board INGV, grazie al suo carattere multidisciplinare, assicura i requisiti di qualità per la pubblicazione dei contributi sottomessi.

MISCELLANEA INGV (MISC. INGV) favours the publication of scientific contributions regarding the main activities carried out at INGV. In particular, MISCELLANEA INGV gathers reports of scientific projects, proceedings of meetings, manuals, relevant monographs, collections of articles etc. The journal is published online to guarantee celerity of diffusion on the internet. A multidisciplinary Editorial Board and an accurate peer-review process provide the quality standard for the publication of the contributions.

**Coordinamento editoriale**

Francesca DI STEFANO  
Istituto Nazionale di Geofisica e Vulcanologia

**Progetto grafico**

Barbara ANGIONI  
Istituto Nazionale di Geofisica e Vulcanologia

**Impaginazione**

Barbara ANGIONI  
Patrizia PANTANI  
Massimiliano CASCONI  
Istituto Nazionale di Geofisica e Vulcanologia

©2025

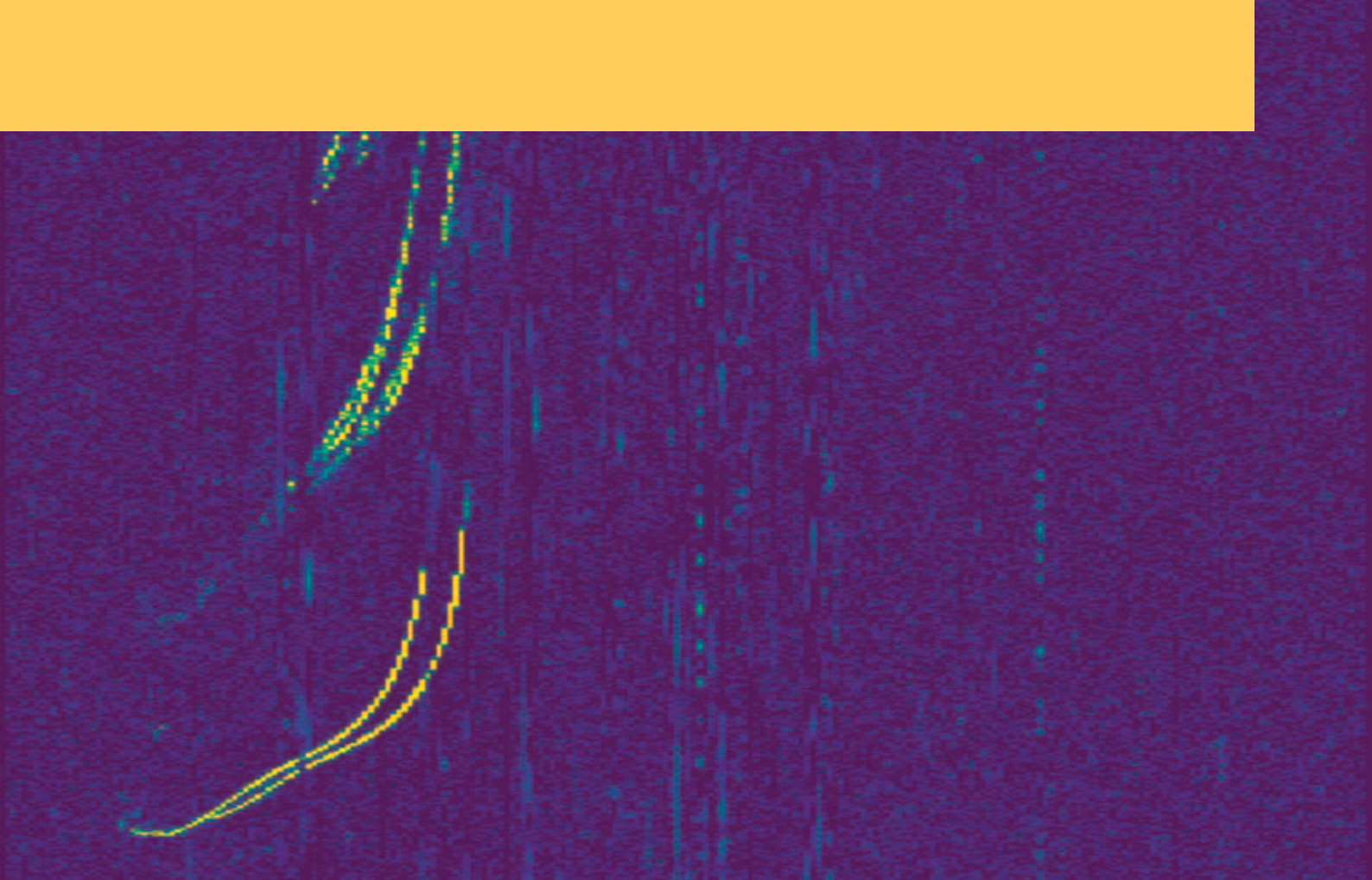
Istituto Nazionale di Geofisica e Vulcanologia  
Via di Vigna Murata, 605  
00143 Roma  
tel. +39 06518601

[www.ingv.it](http://www.ingv.it)



Creative Commons Attribution 4.0 International (CC BY 4.0)





ISTITUTO NAZIONALE DI GEOFISICA E VULCANOLOGIA

